

Spectroscopy, Imaging and Compton-scatter Polarimetry with a Germanium Strip Detector

S.E. Inderhees, B. Philips
Universities Space Research Association, Washington, DC

R.A. Kroeger, W.N. Johnson, R.L. Kinzer, J.D. Kurfess
Naval Research Laboratory, Washington, DC, 20375

B. Graham,
George Mason University, Fairfax, VA

N. Gehrels
Goddard Space Flight Center, Greenbelt, MD 20771

ABSTRACT

Germanium strip detectors combine the excellent energy resolution possible with germanium detectors with fine two-dimensional spatial resolution determined by orthogonal strip electrodes. We are testing a detector with an active volume of $5 \times 5 \times 1 \text{ cm}^3$ and a total of 50 electrodes, 25 on each side with a 2mm pitch. Potential astrophysics applications include use as a focal plane for a coded-aperture telescope in the energy range $\sim 5\text{-}500 \text{ keV}$, as the focal plane of a grazing-incidence telescope in the $\sim 5\text{-}100 \text{ keV}$ band, or in a Compton scatter telescope. The utilization of germanium strip detectors for these applications requires proof of their performance capabilities in terms of energy and spatial resolution, and efficiencies for single and multi-pixel interactions. In this paper, we demonstrate the excellent spectroscopy and imaging performance of a 2mm pitch strip detector, and report on the results of Monte- Carlo simulations of photopeak efficiencies for single and multi-pixel interactions. These simulations show that 2-pixel interactions are a significant fraction of the photopeak efficiency in the 80 - 500 keV range. We demonstrate that these interactions can be used to measure linear polarization of a normally incident beam.

INTRODUCTION

Radiation detectors that combine good energy resolution with fine spatial resolution should find applications in many areas of research. Current challenges in high energy astrophysics require superior spectroscopy to resolve cyclotron features in highly magnetized neutron stars,¹ determine annihilation radiation line-width from the galactic plane,^{2,3} and improve sensitivity to narrow-line features in a variety of astrophysical sources such as supernovae remnants.⁴ Superior angular resolution is needed to localize unknown sources or to resolve closely

spaced sources near the galactic center. Solar flare observations need good spectroscopy to observe the spectral change between thermal and non-thermal emissions.

Applications for germanium strip detectors include coded-aperture imaging where good spectroscopy and high angular resolution are required. Compton scatter telescope imaging^{5,6,7} with sensitivity starting as low as 300 keV would improve on the success of COMPTEL on NASA's Compton Gamma Ray Observatory.⁸ Imaging detectors are needed for the focal plane of a hard X-ray grazing-incidence mirror⁹ that concentrates hard X-rays up to $\sim 100 \text{ keV}$. And finally, position sensitive detectors improve the performance of Fourier telescopes.^{10,11}

In addition to the spectroscopy and imaging capabilities, this detector is sensitive to linear polarization via Compton scattering within the detector. Many applications for polarimetry in γ -ray astronomy have been proposed, for example, a γ -ray polarization measurement of CEN-A would help explain whether the softening of the hard X-ray/ soft γ -ray spectrum is due to Compton scattering,¹² and polarization measurements can elucidate the geometry of accretion disks.¹³ Several Compton-scatter instruments for astrophysics applications have been proposed utilizing scintillating fibers¹⁴, silicon strip detectors¹⁵, and liquid Xenon.¹⁶ Segmented coaxial and planar germanium detectors have been developed

¹Grove, J.E., et al., *Astrophys. J.* **438**, L25 (1995)

²Johnson, W.N., et al., *Astrophys. J.*, **172**, L1 (1972)

³Leventhal, M., et al. *Astrophys. J.*, **225**, L11. (1978)

⁴Clayton, D.D., et al., *Astrophys. J.*, **188**, 155 (1974)

⁵Johnson, W.N. et al., *Imaging in High Energy Astronomy*, Kluwer Press, 1994

⁶Johnson, W.N. et al., *Proc. SPIE* **2518** (1995)

⁷B. Philips, This conference.

⁸Schoenfelder, V. et al., *Astrophys. J. Supplement* **86**, 657.(1993)

⁹Gorenstein, P. et al., *Proc. SPIE* **1736**, 239 (1993)

¹⁰Prince, T.A., et al., *Solar Physics* **118**, 269.(1988)

¹¹Masuda, S., et al., *Nature* **371**, 495. (1994)

¹²J.G. Skibo, C.D. Dermer, R.L. Kinzer, *Astrophys.. J.* **426**, L23-L26 (1994)

¹³P. Mészáros et al, *Apstrophys. J.*, **324**, 1056-1067 (1988)

¹⁴E. Costa, et al. , to appear in *Nucl. Instrum. Meth. A*

¹⁵O'Neill, T.J. et al., *IEEE Trans Nucl. Sci.* **32**, (1992)

¹⁶E. Aprile et al., *Astrophys. J. Supplement*, **92**, 689-692 (1994)

Report Documentation Page				Form Approved OMB No. 0704-0188	
Public reporting burden for the collection of information is estimated to average 1 hour per response, including the time for reviewing instructions, searching existing data sources, gathering and maintaining the data needed, and completing and reviewing the collection of information. Send comments regarding this burden estimate or any other aspect of this collection of information, including suggestions for reducing this burden, to Washington Headquarters Services, Directorate for Information Operations and Reports, 1215 Jefferson Davis Highway, Suite 1204, Arlington VA 22202-4302. Respondents should be aware that notwithstanding any other provision of law, no person shall be subject to a penalty for failing to comply with a collection of information if it does not display a currently valid OMB control number.					
1. REPORT DATE 1995		2. REPORT TYPE		3. DATES COVERED 00-00-1995 to 00-00-1995	
4. TITLE AND SUBTITLE Spectroscopy, Imaging and Compton-scatter Polarimetry with a Germanium Strip Detector				5a. CONTRACT NUMBER	
				5b. GRANT NUMBER	
				5c. PROGRAM ELEMENT NUMBER	
6. AUTHOR(S)				5d. PROJECT NUMBER	
				5e. TASK NUMBER	
				5f. WORK UNIT NUMBER	
7. PERFORMING ORGANIZATION NAME(S) AND ADDRESS(ES) Naval Research Laboratory, 4555 Overlook Avenue, SW, Washington, DC, 20375				8. PERFORMING ORGANIZATION REPORT NUMBER	
9. SPONSORING/MONITORING AGENCY NAME(S) AND ADDRESS(ES)				10. SPONSOR/MONITOR'S ACRONYM(S)	
				11. SPONSOR/MONITOR'S REPORT NUMBER(S)	
12. DISTRIBUTION/AVAILABILITY STATEMENT Approved for public release; distribution unlimited					
13. SUPPLEMENTARY NOTES					
14. ABSTRACT					
15. SUBJECT TERMS					
16. SECURITY CLASSIFICATION OF:			17. LIMITATION OF ABSTRACT	18. NUMBER OF PAGES 5	19a. NAME OF RESPONSIBLE PERSON
a. REPORT unclassified	b. ABSTRACT unclassified	c. THIS PAGE unclassified			

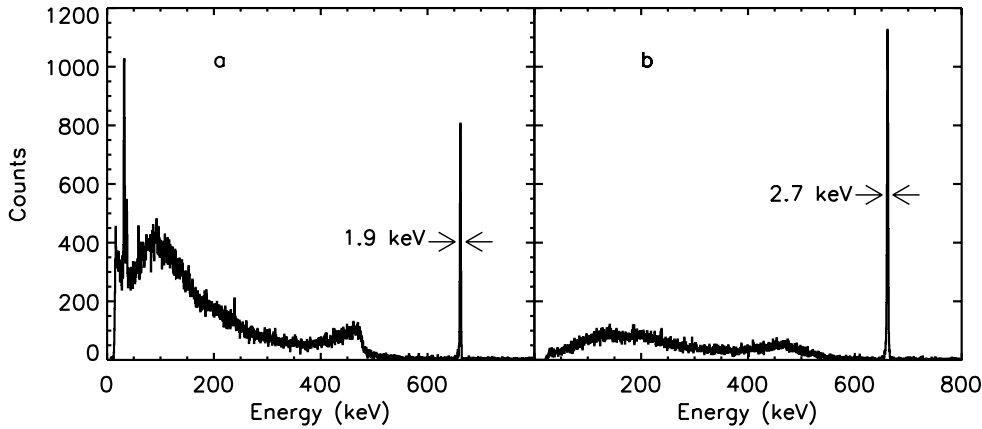


Fig. 1: Energy spectrum from events with signals in a) a single boron strip and b) two boron strips, from a uniform illumination of 662 γ -rays from ^{137}Cs . In the single-strip spectrum, the prominent features are the 662 keV line and the barium K_{α} and K_{β} X-ray lines which are resolved from each other. In two-strip events, the Compton continuum is suppressed. The FWHM is consistent with the additional electronic noise from readout of two strips.

specifically for Compton scatter polarimetry^{17,18} in nuclear experiments. In a typical Compton-scatter polarimeter, efficiency is maximized by using a low-Z scattering element surrounded by an array of high-Z analyzing elements. In the strip detector, any pixel on the detector can be either the scattering or analyzing element, improving the efficiency of the measurement. In the energy range of 100-500 keV, Compton scatters make up a significant fraction of the initial interactions in germanium. For scatters near 90 degrees, the scattered photon's mean free path is greater than 2 mm. In a position-sensitive detector such as described here, this range permits measurement of polarization even when the polarization vector is not aligned with a particular axis of the detector. Therefore, rotation of the instrument is not required when the direction of polarization is unknown.

DEVICE DESCRIPTION

The detector was fabricated¹⁹ by Eurysis Mesures from a crystal of high purity germanium of dimensions $1.1 \times 5.6 \times 5.6 \text{ cm}^3$, with an active volume of 25 cm^3 . The detector is operated at $\sim 80\text{K}$ and is housed in a cryostat with a 1.5 mm thick beryllium window. Orthogonal strip contacts of implanted boron and diffused lithium are deposited on opposite faces of the detector, for a total of 25 strips on each face, with a 2mm pitch. Gaps between strips are 200 μm on the boron side. On the lithium side, gaps between the first nine strips are approximately 600 μm , and 300 μm between the remaining strips. This was done intentionally in order to study the effects of the gap size on the detector

performance. Each strip is connected to a separate readout system consisting of a hybrid preamplifier and a NIM shaping amplifier, and digitized with a 13 bit (boron strips) or 12 bit (lithium strips) ADC. Event-list readout of all strips is triggered by a signal on any boron strip above an adjustable threshold (minimum of 5 keV). Each strip is individually calibrated, and analyzed over an energy range 5-800 keV.

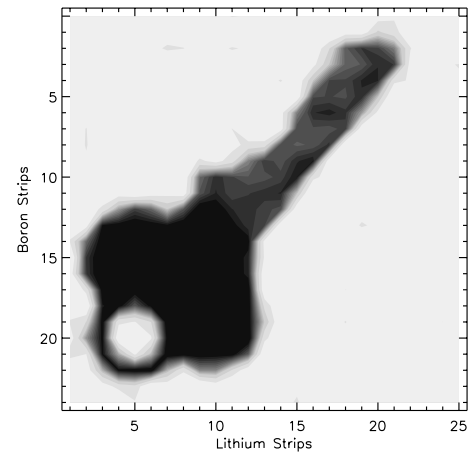


Fig. 2: Shadow image of a brass key using 60 keV γ -rays from ^{241}Am , using single-pixel photopeak data. The background (light area) illumination is ~ 60 counts per pixel. The shaft of the key is thinner than the handle, and therefore absorbs fewer γ -rays.

¹⁷R.A. Sareen, W. Urban, A.R. Barnett, B.J. Varley, Rev. Sci. Instrum. **66** (6), 3653 (1995)

¹⁸A. von der Werth et al., Nucl. Instrum. Meth A **357**, 458-466 (1995)

¹⁹Gutknecht D., et al., Nucl. Instrum. Meth., A **228**, 1 (1990)

ENERGY RESOLUTION AND IMAGING

Detector performance in terms of energy and position resolution and correction for cross-talk effects has been discussed in detail in previous publications,^{20,21} and is summarized here. Cross-talk is negligible on the boron side ($\sim 0.1\%$), but is more significant on the lithium side ($\sim 1.5\%$), due to the greater thicknesses of the contacts ($\sim 300\text{ }\mu\text{m}$ for Li, $\sim 1\text{ }\mu\text{m}$ for boron). The cross-talk fraction for each adjacent strip pair is determined from the position of the 662 keV photopeak for events with signals on the two strips, and a correction applied to the data. When connected individually the FWHM energy resolution at 60 keV is 1.4 keV for the boron strips and 1.7 keV for the lithium strips; at 662 keV the resolution is 1.7 and 2.2 keV, respectively.

Figure 1a shows a ^{137}Cs spectrum of single-strip events on the boron face of the detector. This spectrum was obtained by histogramming the events from all boron strips from a uniform illumination. The photopeak is slightly broader than the 1.7 keV FWHM quoted above, due to slight variations from of the photopeak calibration on each strip, and from the presence of ground loops when all of the strips are connected to the readout electronics. The full-width tenth-maximum (FWTM) response is $\sim 4\text{ keV}$; a Gaussian-distributed peak would have $\text{FWTM} = 1.8\text{ FWHM} = 3.4\text{ keV}$. For the two-strip event spectrum shown in Fig. 2b, peak broadening is consistent with the additional electronic noise from readout of two strips. The good resolution of the photopeak demonstrates the linearity of the energy response of the system. Two-strip events account for 40% of the photopeak events at 662 keV, while single-strip events are 25% of the total.

As a simple demonstration of the imaging capabilities of this detector, we have produced a transmission image of a brass key, shown in Figure 2. This image was produced by illuminating the key with 60 keV γ -rays from ^{241}Am , projecting a shadow onto the detector surface. Single-pixel photopeak (56-62 keV) interactions were selected. The resulting image is normalized by the detector response to a uniform illumination with 60 keV photons. This corrects for the small decrease in single-pixel efficiency for the portion of the detector with wider gaps between the Li strips. Noise is primarily due to counting statistics, with an average of 60 counts per detector pixel in the fully exposed (white) areas. There is more transmission through the shaft of the key, which is thinner than the handle. The excellent energy resolution of this detector allows for rejection of scattered γ -rays, which can add fog to the image. Scatter rejection is particularly effective at energies above 100 keV, where energy loss from Compton scattering usually exceeds a few keV.

EFFICIENCIES FROM MONTE CARLO SIMULATIONS

The utility of this detector for spectroscopic imaging depends on the efficiency of events where the incident pixel can be determined. We have studied the efficiencies of single and multi-pixel interactions in a 2mm pitch germanium strip detector with Monte-Carlo simulations of the detector at energies between 80 and 511 keV. The simulations were performed using EGS4.²² To simulate the actual performance of the detector, the resulting event list is converted into "strip readout" format, i.e. each incident photon produces signals on boron and lithium strips, and multiple interactions in a single strip are summed into one signal. This simple model of the detector does not include the effects of charge-sharing between strips. A Gaussian distributed energy resolution is added to each signal, with a FWHM of 1.5 keV for the boron strips, and 2.0 keV for the Li strips. Finally, a LLD of 5 keV is applied.

Figure 3 shows the results of the simulations for efficiencies of single and double-pixel efficiencies. As expected, the efficiency of single-pixel events falls off rapidly above 100 keV. Two-pixel efficiency is maximum near 150 keV, and drops rapidly with decreasing energy due to the increasing probability of a photoelectric absorption for the first interaction, as well as the shorter mean-free path of the scattered photon. For example a 100 keV photon scattered by 90 degrees produces a 84 keV photon with a mean-free path of 2.2 mm. Above 150 keV, the drop in two-pixel photopeak efficiency is predominantly due the escape of the scattered photon, and the increasing probability of > 2 pixel events.

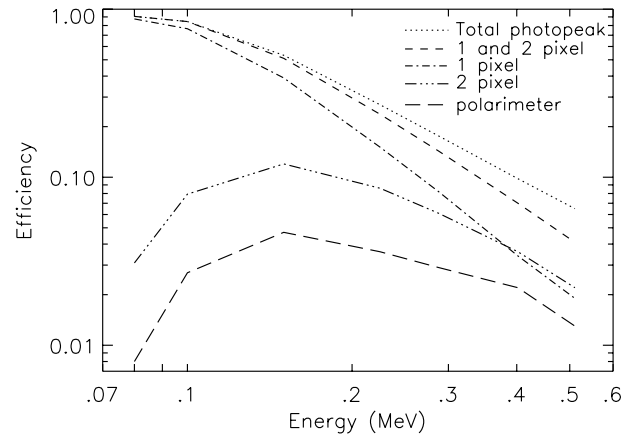


Fig. 3: Efficiencies for single and multi-pixel photopeak events, from Monte-Carlo simulation. The simulation does not include gaps between strips. Also shown is the efficiency of polarimetry events, defined as two-pixel photopeak events in non-adjacent pixels, with Compton-scatter angle $60^\circ < \theta < 120^\circ$.

²⁰Kroeger, R.A., et al., *Imaging in High Energy Astronomy*, Kluwer press, 1994

²¹Kroeger, R.A. et al, *SPIE* **2518**, 236 (1995)

²²Nelson, W.R., Hirayama, H., and Rogers, D., SLAC report 265 (1985)

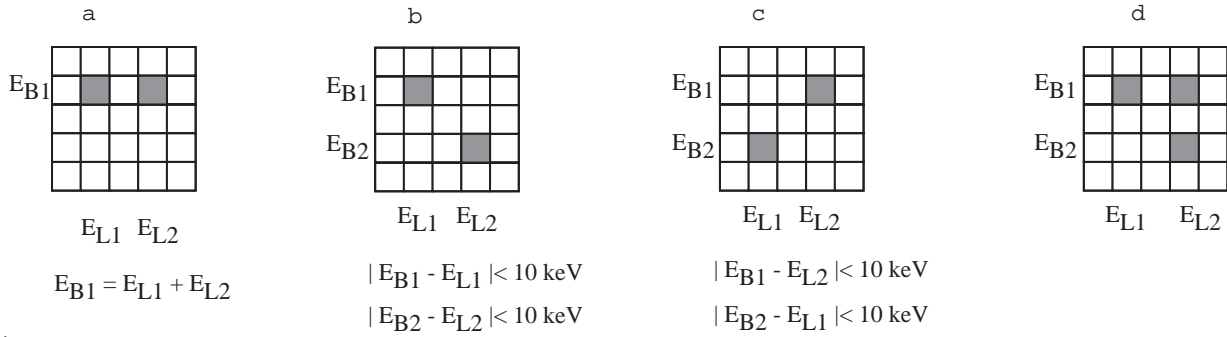


Fig. 4: Pattern of energy deposition in multi-pixel interactions. Reconstruction of interactions along a strip (a) is straightforward. Two-pixel interactions involving 2 strips on each side of the detector (b and c) can be reconstructed and distinguished from three-pixel interactions (d) by the conditions on the readout signals as shown.

COMPTON-SCATTER POLARIMETRY MEASUREMENT WITH TWO-PIXEL INTERACTIONS

In Compton-scatter interactions where the incident photon energy is less than 500 keV, the azimuthal modulation of scattering is maximum for interactions with scattering angle θ slightly less than 90 degrees, shifting to lower θ with higher energies. Therefore the modulation factor of a polarization measurement is maximized by selecting scatters near 90 degrees in the detector, for example between 60 and 120 degrees. The excellent energy resolution of germanium allows selection of these events from the kinematics of the interaction.

We demonstrate a polarization measurement at 290 keV as follows. A partially polarized beam is produced by a 90-degree scatter of 662 keV γ -rays off a 1 cm thick plastic scintillator target located one meter from the germanium detector. A photomultiplier tube detects interactions in the plastic and readout of the strip detector is triggered by a coincidence between the plastic and germanium. The scattered beam is approximately 60% polarized, and normally incident on the germanium strip detector with the polarization vector in the plane of the detector. The scattered beam energy ranges from 279 keV to 294 keV at opposite edges of the detector, due to the small spread in scattering angles about 90 degrees. In addition to the scatter peak there is a background due to accidental triggers on unpolarized background events. The percentage of events under the photopeak that are due to the background is approximately 15%. Thus the selected data are approximately 50% polarized. Separate data sets were acquired with the polarization electric vector aligned parallel to the boron strips ($\phi_0=0$), at 45 degrees relative to the boron strips ($\phi_0=45$), and parallel to the lithium strips ($\phi_0=90$), where ϕ_0 is the angle of the polarization electric vector in the detector coordinates.

After selection of photopeak events, two-pixel interactions are selected from the event list. Figure 4 shows some possible scatter geometries for two-pixel events: a scatter along a lithium or boron strip (a), and a scatter involving two boron and two lithium strips (b and c).

Reconstruction of the scatters along a strip is straightforward. The most common two-pixel Compton-scatter interaction involves two strips on each side of the detector, and it is necessary to analyze the pattern of energy deposition to determine which pixels are involved in the event. To reconstruct these scatters, we require that the energies differ by less than 10 keV. For example, for the case shown in Figure 4b, we require $|E_{B1} - E_{L1}| < 10$ keV and $|E_{B2} - E_{L2}| < 10$ keV. If the energy matching conditions of Figure 4b or c are not met, the event is assumed to be a three-pixel interaction (Figure 4d). Two-pixel events between pixels that share an edge are rejected for polarimetry (these events have a high fraction of photopeak interactions in the gaps between the strips).

Next, scatters with $60 < \theta < 120$ degrees are selected from the kinematics of the interaction using the Compton scatter formula. In this energy range, the incident pixel is most likely the one with lower energy deposition.²³ Note that this assumption is always valid for $E < 255.5$ keV, and where there is only a single interaction in the first pixel. Above 255.5 keV, an increasing fraction of events will have a larger energy deposition in the incident pixel.

Figure 5 shows the angular variation of the polarization ratio in the detector plane, defined as $R = (N_{\perp} - N_{\parallel}) / (N_{\perp} + N_{\parallel})$, where N_{\perp} is the number of photons scattered along an axis perpendicular to ϕ , and N_{\parallel} is the number scattered along the axis parallel to ϕ . The data are binned into a range of angles about ϕ . For visual effect the results are plotted for a full 180 degrees; only the first four data points of each plot are independent. For $\phi_0 = 0, 45, 90$ degrees we find $R = 0.32 \pm 0.02, 0.30 \pm 0.01$ and 0.41 ± 0.05 respectively. Taking the incident beam to be 50% polarized, this gives a modulation factor of 0.6-0.8. The higher measurement for $\phi=90$ indicates there is some asymmetry of the response of the detector. Asymmetries in the polarization response can be determined by calibration with an unpolarized beam.

²³J.E. Naya Ariste, F. Albernhe and G. Vedrenne, Nucl. Instrum. Meth. A, **357** (1995), 170-177

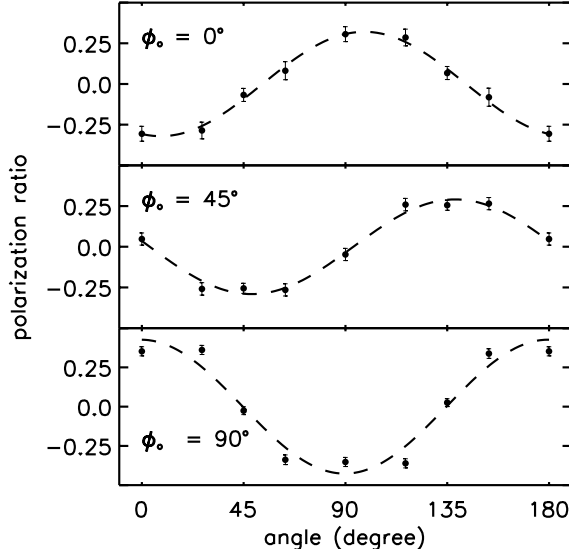


Fig. 5: Polarization ratio as function of ϕ , where ϕ is defined relative to the boron strips of the germanium detector with the polarization electric vector aligned a) parallel to the boron strips, b) at 45 degrees relative to the boron strips and c) perpendicular to the boron strips.

Figure 3 shows the efficiency of a polarimetry experiment calculated from the Monte-Carlo simulations (i.e. the efficiency of photopeak absorption with a scatter between non-adjacent pixels, where the kinematics are consistent with a 60-120 degree scatter). In the above experiment, 11% of the photopeak data are used to measure polarization at 290 keV. Assuming a total photopeak efficiency of 20%, this yields a polarimetry efficiency of 2.1% of the incident photons. For comparison, the Monte-Carlo simulation gives an efficiency of 2.9%.

CONCLUSIONS

We have demonstrated that good spectroscopy and imaging can be obtained with germanium strip detectors. The spectral resolution is maintained even for events where energy is deposited in more than one strip of the detector. Monte-Carlo simulations show that the photopeak efficiency for one and two pixel events is comparable to the photopeak efficiency of a non-segmented planar germanium detector for energies < 500 keV. The results of the polarimeter measurement are quite promising, with good efficiency and modulation factor, and demonstrate our ability to reconstruct the more complicated two-pixel events. In future work, we will add the inter-strip gaps to the Monte-Carlo analysis, for a more realistic modeling of the detector performance.

This work was supported in part by the Office of Naval Research and NASA under contract No. W-18486.